Geophys. J. Int. (2013) doi: 10.1093/gji/ggt336
Geophysical Journal International Advance Access published October 3, 2013

Palaeomagnetism of Palaeozoic glacial sediments of Northern Ethiopia: a contribution towards African Permian palaeogeography

Tesfaye Kidane,[1,2] Valerian Bachtadse,[2] Mulugeta Alene[1] and Uwe Kirscher[2]

[1] *School of Earth Science, College of Natural Science, Addis Ababa University, P.O. Box* 1176, *AA, Ethiopia. E-mail: tesfayek@yahoo.com*
[2] *Geophysics Section, Department of Earth and Environmental Sciences, LMU, Germany*

Accepted 2013 August 20. Received 2013 August 16; in original form 2013 April 3

SUMMARY

One hundred fourteen oriented palaeomagnetic core samples were collected from 13 palaeomagnetic sites on subhorizontal to tilted glacial sediments at five localities of Northern Ethiopia. Combined alternating field (AF) and stepwise thermal demagnetization techniques were successfully applied to resolve the complete directional spectrum. A viscous remagnetization (VRM) and one stable component of magnetization were identified in most of the specimens. The VRM is removed between a temperature range of 120–350 °C and AF of up to 30 mT. Further heating until ∼650 °C results in smooth decay of the natural remanent magnetization (NRM) intensity to about 50 per cent and the rest of the NRM is efficiently removed by heating to 690 °C, while only 30–50 per cent of NRM is removed by the maximum AF available suggesting haematite as remanence carrier. Results of the magnetization decay curve plots and rock magnetic analyses using the variable field translation balance indicated the presence of magnetite with minor goethite, pyrrhotite as well. The high stability component defining a straightline segment, starting 350 °C and/or 30 mT is mostly directed towards the origin and interpreted as the characteristic remanent magnetizations (ChRMs). The direction of magnetization is determined both by best-fitting line using the least-square technique of Kirschvink and remagnetization circles of Halls for few unresolved overlapping components. The site mean directions of the sediments from two sites are normal polarity and are close to present-day field directions at the sample site. The site mean directions from 11 sites, on the other hand, are reversed in polarity with better grouping in the tilt-corrected coordinate and pass the McFadden fold test. This overall site mean direction is Dec = 143.4°, Inc = 58.8° ($N = 11$, $\alpha_{95} = 9.7°$) with a corresponding mean pole position of Lat = 26.0°, Lon = 249.5° ($N = 11$, $A_{95} = 13.1°$). This geomagnetic pole position is later rotated into West Africa coordinates to allow for extensional rifting in the Benue Trough about an Euler pole position, at 19.2°N, 352.6°E through an angle −6.3° (clockwise). The resulting pole position is located at ϕs = 246.6°E, λs = 31.8°S ($N = 11$, $A_{95} = 13.1°$), this pole with its 95 per cent confidence circle intersects the 270–310 Ma, segment of the APW path for West Africa consistent with ages of between late Carboniferous and early Permian. The result also implies that the Late Carboniferous Dwyka land ice sheet had probably extended more than 1000 km further north to Ethiopia than previously known.

Key words: Plate motions; Palaeomagnetism applied to tectonics; Rock and mineral magnetism; Africa.

1 INTRODUCTION

There is an ongoing debate about palaeogeographic configurations of Pangea in the Late Palaeozoic Era (e.g. Van der Voo 1993; McElhinny & McFadden 2000; Muttoni *et al*. 2003; Domeier *et al.* 2012). A comprehensive and detailed historical development of Pangea reconstruction and the opposing arguments in the Palaeozoic Era has recently been given elsewhere (Domeier *et al*. 2012) and briefly presented below.

At least two competing palaeogeographic reconstructions models have been proposed over the years; Pangaea A and Pangaea B. Reconstruction type A is a slight modification of the original Wegener's (1915) reconstruction. It has widely been accepted as the likely configuration in the Early Jurassic just prior to the opening of the

Atlantic Ocean (Van der Voo 1993); because of the perfect matching of conjugate seafloor magnetic anomalies and marine fracture zones across the Atlantic (e.g. Klitgord & Schouten 1986) and supported by palaeomagnetic data for Early Jurassic (Irving 1977). However, its validity was later disputed (Irving 1977; Kanasewich *et al*. 1978; Morel & Irving 1981). Irving (1977) has demonstrated the existence of significant difference between the reference latitudes of Laurasia and Gondwana for pre-Jurassic time with a profound implication that Gondwana must have been farther north, relative to North America, than its position in the Pangea A configuration, during the Permian and the Triassic. Consequently, significant crustal misfit and overlap (>1000 km) between Laurasia and Gondwana results; to eliminate this overlap, a relative eastward translation of Gondwana of ∼3500 km was unavoidable.

In order to resolve this paradox, a new palaeogeographic reconstruction, named as type B, was introduced by Irving (1977) and with further additional palaeomagnetic data, the necessity of type B reconstruction hypothesis and its validity for Carboniferous to Triassic (Kanasewich *et al*. 1978; Morel & Irving 1981) was asserted. Reconstruction type B, however, could not gain wider acceptance by the geosciences community, owing to the fact that available geological and geophysical data overwhelmingly assert that the Atlantic Ocean opened from Pangea A position. This would require Pangea B to transform to Pangea A in the Permian to Late Triassic (Van der Voo 1993; McElhinny & McFadden 2000; Muttoni *et al*. 2009). The skepticism on the Pangea B configurations by many geoscientists lies on the integration of suspicious poor-quality palaeomagnetic data with poor age control from red beds of South America and Africa and potential inclination error from inclination shallowing in sediments potentially produce latitudinal artefacts (Rochette & Vandamme 2001; Muttoni *et al*. 2003).

2 GEOLOGICAL SETTING OF THE PALAEOZOIC DIAMICTITE OF TIGRAI

Patchy exposures of diamictite consisting of lithified, poorly sorted terrigenous glacial sediments, are found in different parts of the Tigrai region (Northern Ethiopia). This diamictite constitutes a distinctive succession of strata between the underlying a late Proterozoic, low-grade basement rocks of the Arabian Nubian Shield (ANS) and overlying Mesozoic sedimentary sequences. The glaciogenic sediments, initially identified as bluish–pink shale that outcrop west of Adigrat town (Blanford 1869, 1870), were regarded as part of the Mesozoic sedimentary sequences (Mohr 1965). Merla & Minucci (1938) had described them as red brick to black lenses of shale outcrops near Adigrat and south of Hauzien; also noted occurrences of beds of conglomerate with big pebbles.

Dow *et al*. (1971) were the first to identify the glacial origin of these rocks, with detailed lithological descriptions and regional correlations recognized it as tillite. They differentiated glacigenic sandstone and tillite facies, which are named as 'Enticho Sandstone' and 'Edaga Arbi Glacials', respectively (Beyth 1972a,b, 1973). The tillites make up 10 per cent of the whole Palaeozoic sequence and were laid down in N–S trending furrows (Beyth 1972b). The age of these sediments has so far not been accurately determined. A precise stratigraphic assignment is not possible because of the lack of age diagnostic fossils, and hence their regional stratigraphic position remains ambiguous. Consequently, they have been attributed either to the extensive Ordovician glaciation centred in southern Algeria (Beuf *et al*. 1971; Vaslet 1990; Semtner & Klitzsch 1994; Clark-Lowes 2005; Moreau *et al*. 2005), or to the early Permian—late Carboniferous glaciation centred in southern Africa (Karroo, Du Toit 1953; Furon 1963). Dow *et al.* (1971) and Saxena & Assefa (1983), based on rare fossil Siphonoromid impressions within the Edaga Arbi Glacials, provided the first supporting evidence for an Ordovician age. This Palaeontological argument was later questioned (Sacchi *et al*. 2007), who stated that an alternative interpretation of these findings was equally compatible with a late Permian age. In addition, Beyth (1972a) referring to a palynologic analysis of the Edaga Arbi Glacials suggested 'not older than Devonian'.

In an attempt to determine the age of the Edaga Arbi Glacials and the Enticho Sandstone palaeomagnetically, Shackleton & Lomax (1974) published results from two non-procedural hand samples from Enticho and Fincha, respectively, yielding palaeomagnetic pole positions at 293°E longitude, and 32°N, latitude with $A_{95} = 27.0°$ for Enticho and 250°E longitude and 35°N latitude with $A_{95} = 3.0°$, respectively. These results were correlated with the Tanzanian red beds of early Permian age (McElhinny *et al.* 1968). This report was based on non-demagnetized data and not fulfilling any of the palaeomagnetic quality criteria such as the ones proposed by Van der Voo (1993). Their obtained pole therefore is of limited use. Bussert & Schrank (2007) based on Palynomorphs identified and extracted from the glacigenic sediments assigned an age of latest Carboniferous—early Permian period to the Tillite and upper part of Enticho Sandstone. However, they concluded that the lower part of the Enticho Sandstone is an older sedimentary unit with an age of upper Ordovician equivalent to those in Eritrea.

Sacchi *et al*. (2007) discovered volcanic pebbles in the diamictite sequences in Hauzien—Megab (HM), Mai Kenetal—Edaga Arbi (MK), which they considered as a supporting evidence for a Permian age on the grounds of regional geology. However, their assumption is inconsistent with regional/global tectonics as the mid-Permian to Middle Triassic was a tectonically stable interval (e.g. Hallam 1983; Smith & Livermore 1991).

The purpose of this palaeomagnetic study is to determine the age of deposition of these sediments and to distinguish which one of the two possible ages described earlier is right. This will be done by comparing the results of the palaeomagnetic pole position obtained from the study with the African apparent polar wander path (AAPWP) curve (Besse and Courtillot 2002; McElhinny *et al*. 2003; Torsvik *et al*. 2008; Torsvik *et al*. 2012). For this purpose, we have collected samples from Negash, Hauzien–Megab–Koraro (HMK), Enticho and Edaga Arbi areas (EDAa) of Tigrai region in Northern Ethiopia.

3 PALAEOMAGNETISM

3.1 Sampling

During two sampling seasons, 114 palaeomagnetic core samples from 13 different palaeomagnetic sites covering five geographic locations (Enticho, HMK, Edaga–Arbi type area, Negash and its surroundings, Fig. 1) were collected using a portable gasoline powered drill. During the first sampling season, samples were collected from Enticho which are coded as Enticho Palaeozoic sandstone (EPSST) and NPSST); while during the second season samples were collected from Negash village in the Belessa area, EDA and HMK area coded, respectively, as Negash–Belessa sandstone (NBLS), EDA and HMK area. All samples were oriented with a standard magnetic compass. Each palaeomagnetic site covers a different stratigraphic

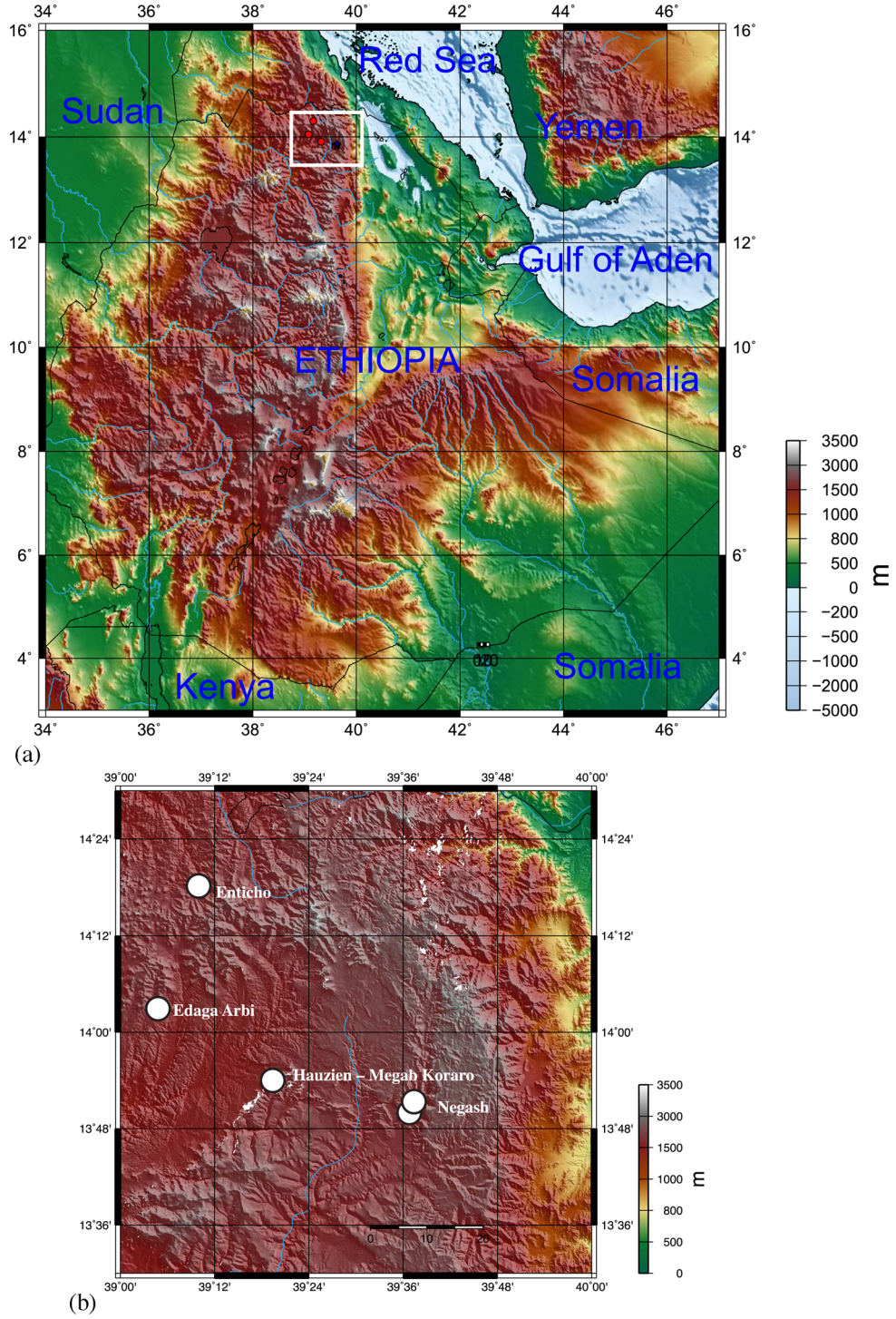

Figure 1. (a) Digital elevation map (DEM) of Ethiopia and surrounding regions, white rectangle shows locations of the studied area in Tigrai region. (b) A blow-up DEM showing details of white rectangle, that is, geographic locations of study sites. (c) A representative picture to show outcrop patterns of the Palaeozoic and Mesozoic Sediments.

level within the two glaciogenic sediments. In the Negash area, exposures of distinctive greyish coloured and thinly stratified dipping beds (strike/dip—130°/27°SW) of the Edaga Arbi Glacials are exposed just below the steep slope forming Triassic aged 'Adigrat Sandstone'. A prominent E–W trending fault upthrown the underlying basement rocks to the north. A valley that developed later between the basement (north) and sediments (south) along this E–W running fault line exposes a cross-bedded (with orientation of cross-bed, 120°/12°NE) medium to coarse-grained whitish coloured tilted (095°/16°SW) sandstone beds adjacent to the Edaga Arbi Glacial rocks at Negash Belessa site. A total of six sites, four from the Edaga–Arbi Glacial strata and two from Enticho Sandstone beds were collected. In the HMK, along a spectacular geomorphologic outcrop of the steep slope forming Adigrat Sandstone and

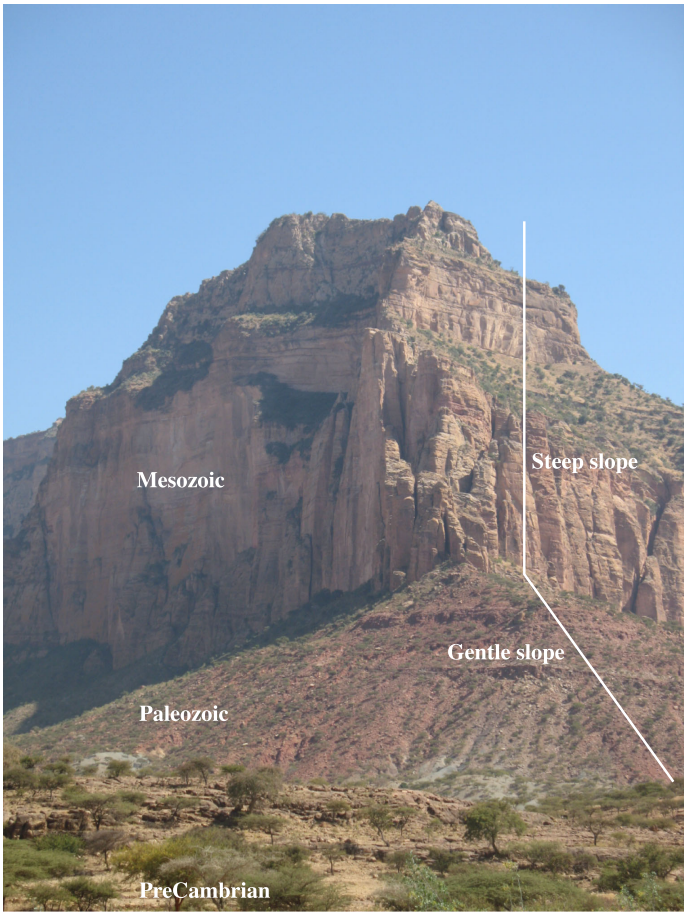

(c)

Figure 1. (*Continued.*)

the gentler slope forming Edaga Arbi Glacials (Fig. 1c), two sites were collected from the Edaga Arbi Glacial facies with flat lying attitudes. In the Enticho-type area, palaeomagnetic sampling was carried out at the bottom of the section from two stratigraphic levels, where finer-grained beds were identified. Finally, three sites from the Edaga Arbi facies near the Edaga Arbi village (Figs 1a–c) were collected.

3.2 Laboratory analyses

A total of 190 specimens out of the 228 specimens prepared from the 114 samples were measured. Both thermal (TH) or alternating field (AF) demagnetization techniques were used in order to resolve the directional spectrum. In addition, representative samples were used to determine the rock-magnetic properties. All palaeomagnetic and rock-magnetic experiments were carried in the Palaeomagnetic laboratory facility at Ludwig-Maximilians-Universität München. Pilot samples were demagnetized thermally in 22 steps from room temperature up to 700 °C as well as in AFs from 0 to 100 mT in 13 steps. Demagnetization steps during routine laboratory procedures were reduced to 11–15 steps.

3.2.1 Rock magnetic properties

Six representative specimens from rocks of the glaciogenic and sandstone facies were subjected to isothermal remanent magnetization (IRM) experiments (Fig. 2a). An initial steep rise in IRM up to an applied field of ∼300 mT is observed in all samples. A further steep (e.g. NPSST2-6B, Type B) or less steep (e.g. NPSST3-7B, Type C) increase in intensity was observed in some samples in fields up to ∼500 mT. None of the samples studied reaches saturation at maximum fields of 2250 mT. The rapid increase in intensity in magnetizing fields of up to 300 mT is diagnostic for magnetite, whereas the fact that no saturation is achieved at external fields of 2250 mT points towards the presence of a second, high coercive magnetic phase very likely to be haematite and/or goethite AF demagnetization of the IRM supports this interpretation. Depending on the type of IRM acquisition (rapid gain in intensity at low external fields versus significant gain in intensity at higher external fields), AF demagnetization is successful in removing between 10 and 70 per cent of the total IRM. This generally indicates that most of the specimens are characterized by a high h_c magnetic mineral(s) and probably significant contribution of haematite (Fig. 2b).

3.3 Microscopic properties

Petrographic analysis was carried out using reflecting light microscope on selected polished surfaces of cylindrical samples, and oil immersion for the highest magnification. Observation under microscope reveals that the opaque minerals make up less than 5 per cent of the total material and in almost all cases identical optical properties are observed. Magnetic grains have lamellae with clear banding of haematite (white—thicker stripe) and ilmenite (dark grey in

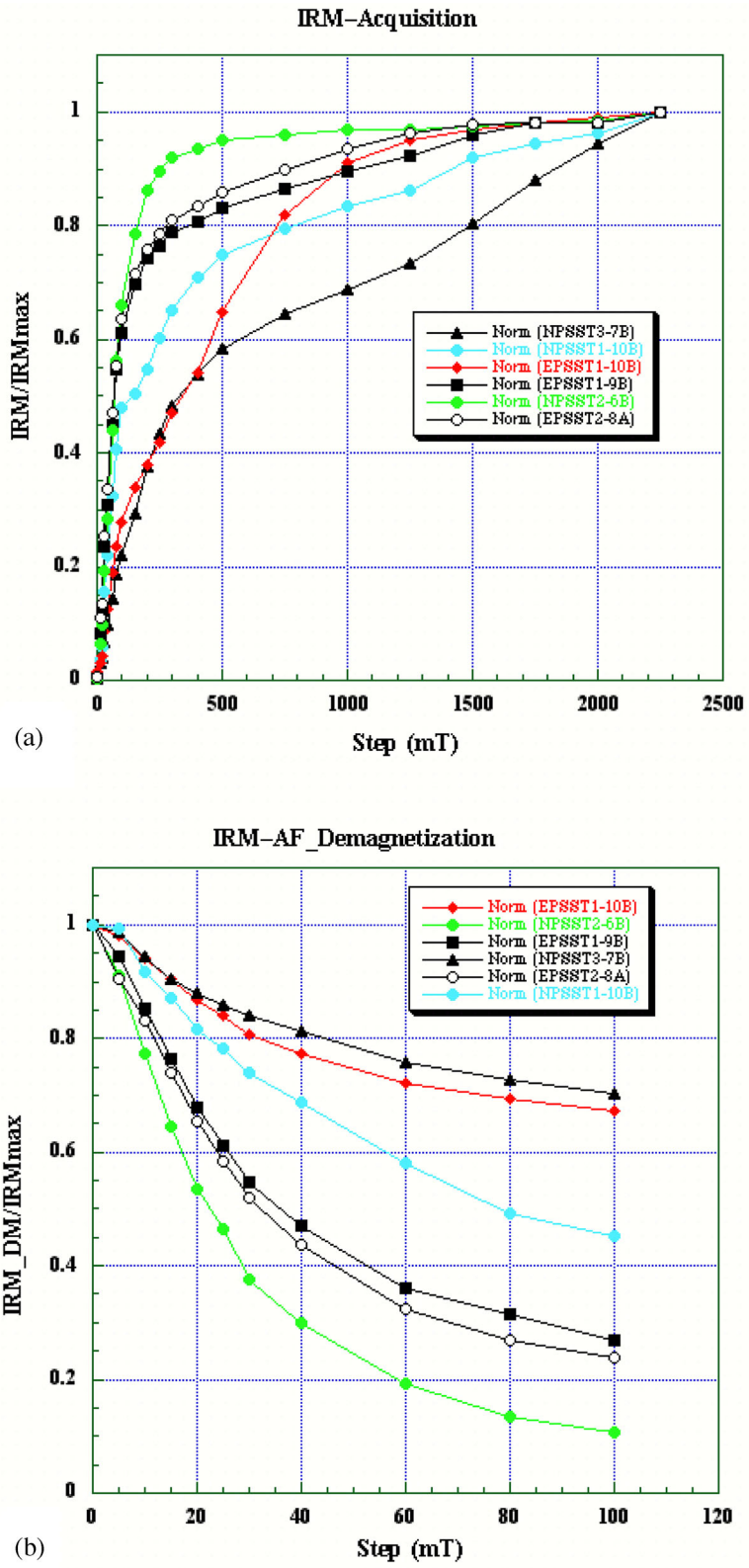

Figure 2. (a) IRM acquisition experiment for representative specimens from Edaga Arbi Glacial and Enticho Sandstone facies. (b) AF demagnetization curve of the IRM experiment in (a), the corresponding specimens names are given for each colour codes.

Figs 3a–c) as the dominant magnetic mineralogy. The size of these grains is mostly lower than 2 μm, but can reach up to 2.5 μm (Fig. 3). The second case is where magnetite (brighter whitish lamellae) and hemo-ilmenite (grey lamellae) in which both show birefringent fine alteration products (possibly calcite and sericite) and also a yellow bright surface possibly sulphide alterations indicting possible existence of iron sulphides as well (Fig. 3d). The magnetic grain size ranges (Fig. 3, compare using given scale) are consistent with

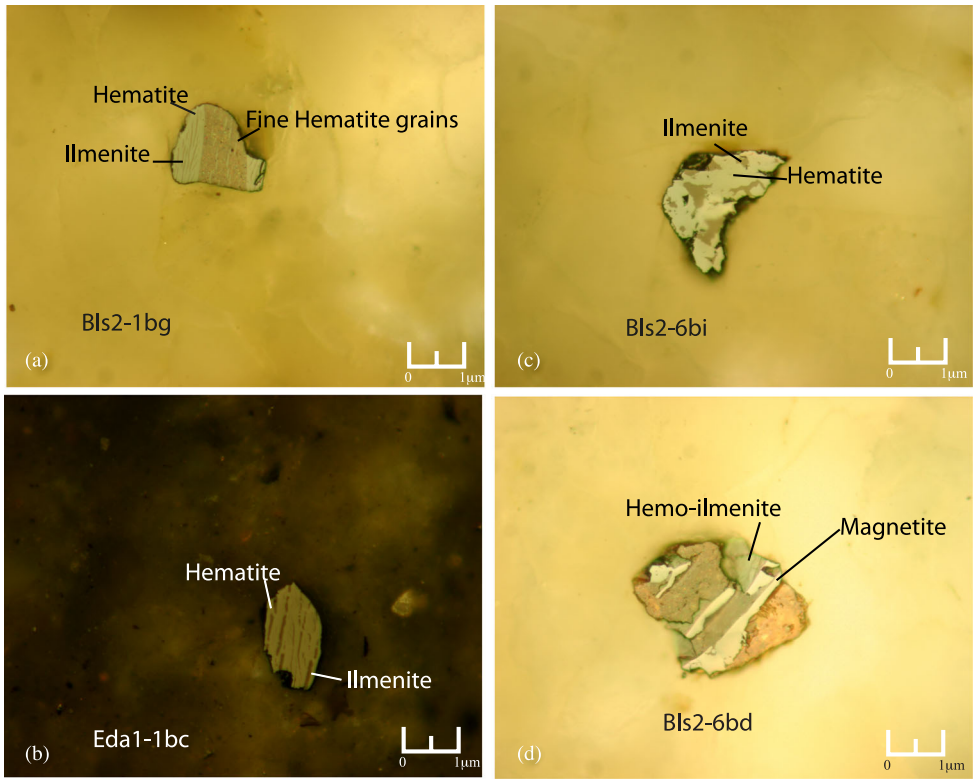

Figure 3. Observation under the highest magnification (50×) objectives with oil immersion: (a) grain showing lamellae of haematite and ilmenite as bands, with fine haematites spots; (b) haematite and ilmenite lamellae forming bands; (c) irregular haematite (grey colour); (d) hemo-ilmenite and magnetite (light grey) with bright non-opaque materials (alteration products), some have yellow fresh surface (probably sulphides).

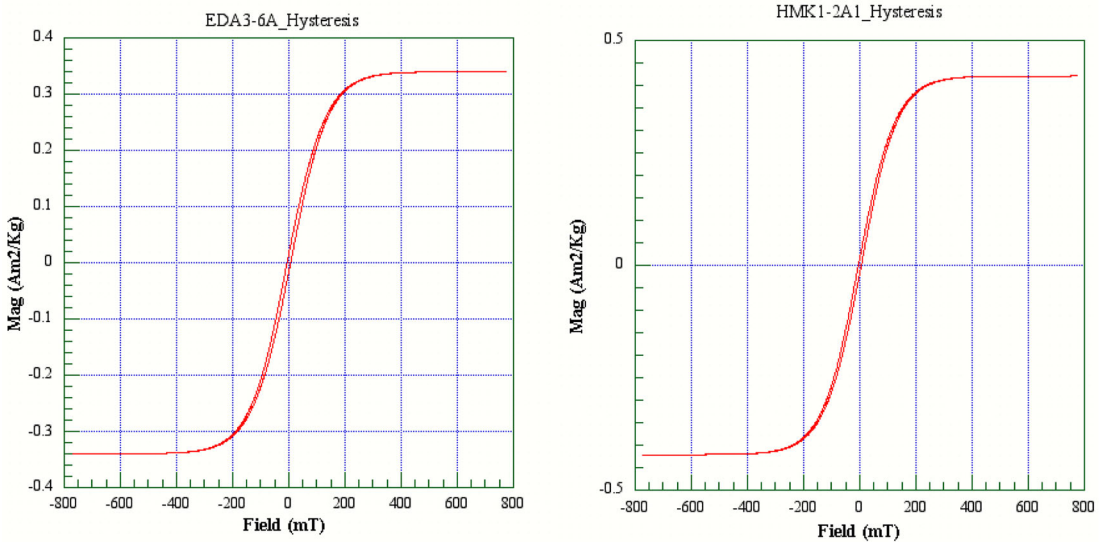

Figure 4. Hysteresis cycles with effect of paramagnetism corrected for representative specimens, all measured specimens show narrow loop with typical low remanent saturation magnetization.

single-domain (SD) haematite and its alterations and multidomain (MD) grains of magnetite.

3.4 Hysteresis and thermomagnetic curves

The hysteresis cycles and thermomagnetic curves were measured using the variable field translation balance (Krasa *et al*. 2007) in order to better distinguish between the coexisting magnetic materials. The hysteretic cycles of all measured specimens show typical loops with rapid rise until applied fields of 200 mT followed by a gradual increase up to external fields of 300 mT. At applied fields of higher than 300 mT, most of the specimens reached their saturation (Fig. 4). The behaviours of all samples are identical and characterized by a distinctive narrow loop with very small amounts of remanent saturation, which is indicative of the presence of MD magnetic grains. The thermomagnetic experiment was carried out for the same number of representative samples. The samples were heated to 700 °C under field-free conditions. In these samples, the

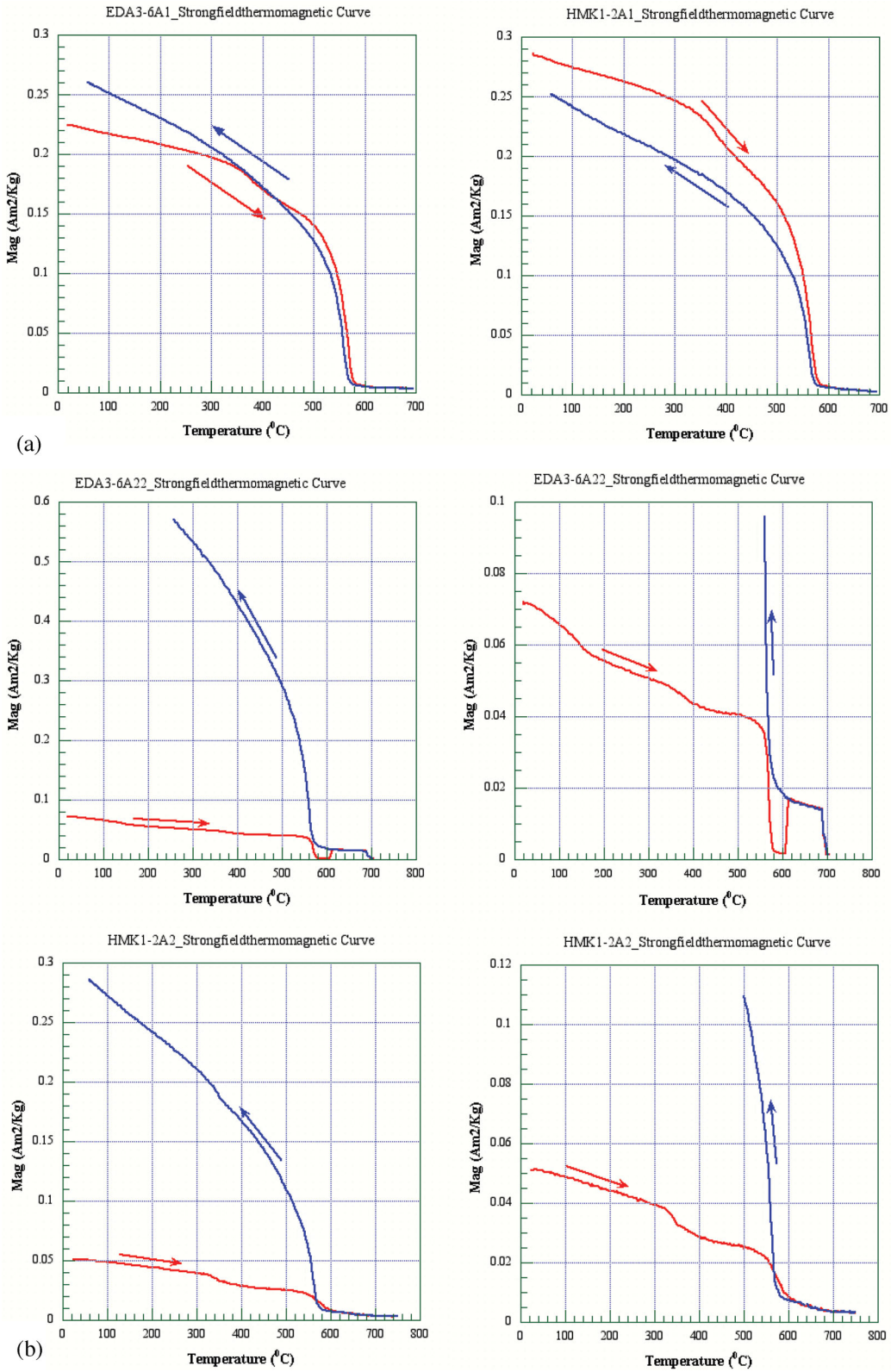

Figure 5. (a) Thermomagnetic curves for representative samples both with irreversible curves. Specimens EDA3-6A1 & HMK1-2A1 show their cooling curve (blue) having higher and lower saturation magnetization, respectively, than the initial magnetizations. Both also show consistent two inflections, one between 300 and 400 °C and the second one at 580 °C possibly corresponding to pyrrhotite and magnetite magnetic mineralogy. (b) Left column shows thermomagnetic curves for representative samples with low applied field (0.2 A) at low temperatures till 630 °C for the upper row, and till 550 °C for the lower row; and higher fields of 5 A for both at temperature higher than the given and during cooling process. The right column shows a blow-up of the left columns for low saturation magnetization values to see details. Upper column shows four distinct Curie temperatures, 120, 350, 580 and 680 °C, while the lower column is consistent with three Curie temperatures, 350, 580 and 680 °C.

heating and cooling curves are not reversible with two clear inflections, one around 350 °C and a second one at around 580 °C (Fig. 5a). The curve is irreversible in some cases with the cooling curve ending at higher (specimen EDA3-6A1, Fig. 5a) or lower (specimen HMK1-2A1, Fig. 5b) saturation magnetizations (j_s) than the starting magnetization. These inflection points correspond with Curie temperature estimates of goethite and pyrrhotite converting to haematite or magnetite after heating to 700 °C. However, in all cases, the magnetizations dropped to zero at 600 °C of the heating cycle suggesting dominance of magnetite and scarcity of haematite in the thermomagnetic experiments. This observation is inconsistent with the predominance of haematite in the IRM experiments and in NRM intensity decay curves. Contribution of magnetite in the remanence results was observed, only in the Enticho sandstones samples at Negash that recorded secondary magnetizations. In order to understand the reasons why magnetite dominant in the thermomagnetic experiments and haematite is nearly absent, supplementary measurements were made on more specimens. The specimens were subjected to a weak field of 7.4 mT during the heating cycle up to 550–630 °C and a stronger field of 148 mT at higher temperatures; during the cooling cycle, the same strong field was maintained throughout the process. Results indicate three to four inflections with Curie points at 120° (only for EDA3–6A22, Fig. 5b), 350, 580 and 680 °C. These inflection points are consistent with Curie temperatures of goethite, pyrrhotite, magnetite and haematite. This indicates that the j_s during thermomagnetic experiments may have been swamped by MD magnetite (strong—j_s), which does not appear in remanence record and concealed the haematite (small—j_s) signal, a major remanence contributor of the studied rocks. In most samples, the remanence carrier haematite has a Curie temperature of around 685 °C indicating pure haematite (Fig. 5b—specimen EDA3–6A22) but in few cases, it shows a gradual decrease in magnetization between 600 and 700 °C (Fig. 5b—specimen HMK1–2A2).

4 PALAEOMAGNETIC DIRECTIONS

Routine palaeomagnetic directional measurements for most specimens treated by both TH and AF techniques resulted in a clear and well-defined single component of magnetization with a secondary component whose blocking temperature spectra are partly overlapping (Figs 6a–c). Representative Zijderveld diagrams (Figs 6a–c) are given from the two glaciogenic facies at three different geographic locations, Edaga Arbi, Enticho and from HMK areas,

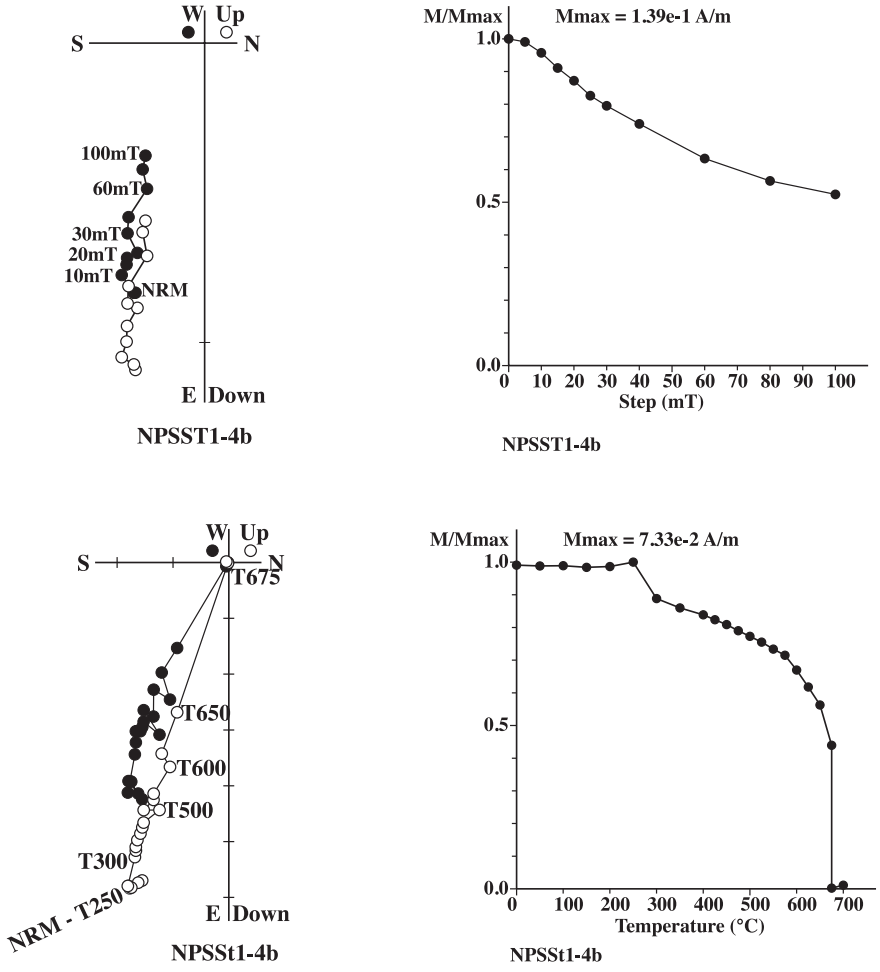

(a)

Figure 6. Examples of Zijderveld diagrams for twin specimens treated by AF and TH from representative geographic locations and Glacial facies (a) from Edaba Arbi Glacials at Negash, (b) from Enticho sandstone at Enticho and (c) from Edaga Arbi Glacials at Hauzien–Megab Koraro sampling areas. In all the studied specimens, the magnetic polarity is down and pointing south consistent with reversed configuration.

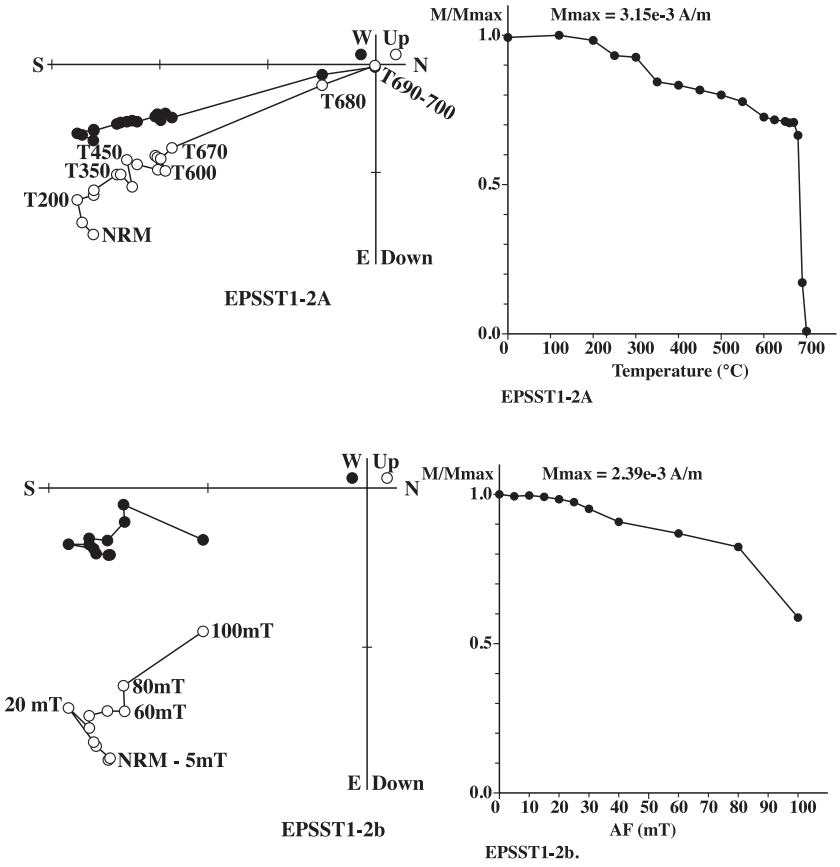

(b)

Figure 6. (*Continued.*)

respectively. The first and low stability component which does not necessarily define directions is usually removed by heating to ~300 °C or subjecting to AF of <20 mT. However, for some samples, this component resists until higher temperatures and AF fields. The second and high stability component starts to be isolated by heating above 350 °C or AF of ~30 mT. During thermal demagnetization, only ~30 per cent of magnetization is removed by heating up to 600 °C, whereas the remaining 70 per cent is removed between steps at temperatures of up to 690 °C. Only ~50 per cent of NRM is removed by AF of 100 mT (the maximum demagnetizing field available in the laboratory). However, the direction of magnetizations at high temperature and high demagnetizing fields is similar to the direction isolated at lower steps of demagnetizations greater than 35 mT and above 350 °C. The high unblocking temperatures as well as the high-coercivity components have similar directions and define linear segment directed towards the origin, which are interpreted as characteristic remanent magnetization (ChRM). In cases, the high stability component has unresolved overlapping spectra and unblocking temperatures and no stable linear segments were obtained. The direction of magnetization for specimens with multiple components have overlapping spectra and unblocking temperatures is determined by remagnetization circles of Halls (1976, 1978), while for those with stable straight line segments is determined by the best-fitting line using the least-square technique of Kirschvink (1980).

4.1 Site mean directions

The directions of magnetizations from sample to sample, site to site and one location to the other shows some differences probably very likely to reflect secular variation. The directions of magnetizations determined by either principal component analysis or remagnetization circles techniques are used to determine the site mean

Site mean directions at site level and overall mean direction are calculated by using Fischer (1953) statistics for those having stable endpoints and McFadden & McElhinny (1988) statistics for combined stable endpoints and great circles using palaeomac software (Cogné 2003). The site mean directions of 11 sites in *in situ* coordinates are given with two sites in grey colour from the Enticho Sandstones at Negash area, which are judged remagnetized and excluded from further analyses (Fig. 7). The red coloured stars stand for the overall mean directions in the *in situ* (Fig. 7a) and tilt-corrected coordinates (Fig. 7b).

The resulting site mean directions from the 11 sites from the four areas studied are exclusively of reversed polarity, which corresponds to the Kiaman-reversed period and only two sites from the Enticho sandstone in Negash area are of normal. However, since the *in situ* mean directions of the two normal sites are close to the direction of the present-day field in the sampling area, while the tilt-corrected coordinate mean moves away from it to unrelated position. Due to this, they are considered to be results of recent remagnetizations. The remaining 11 sites (Table 1) have been averaged and an overall *in situ*

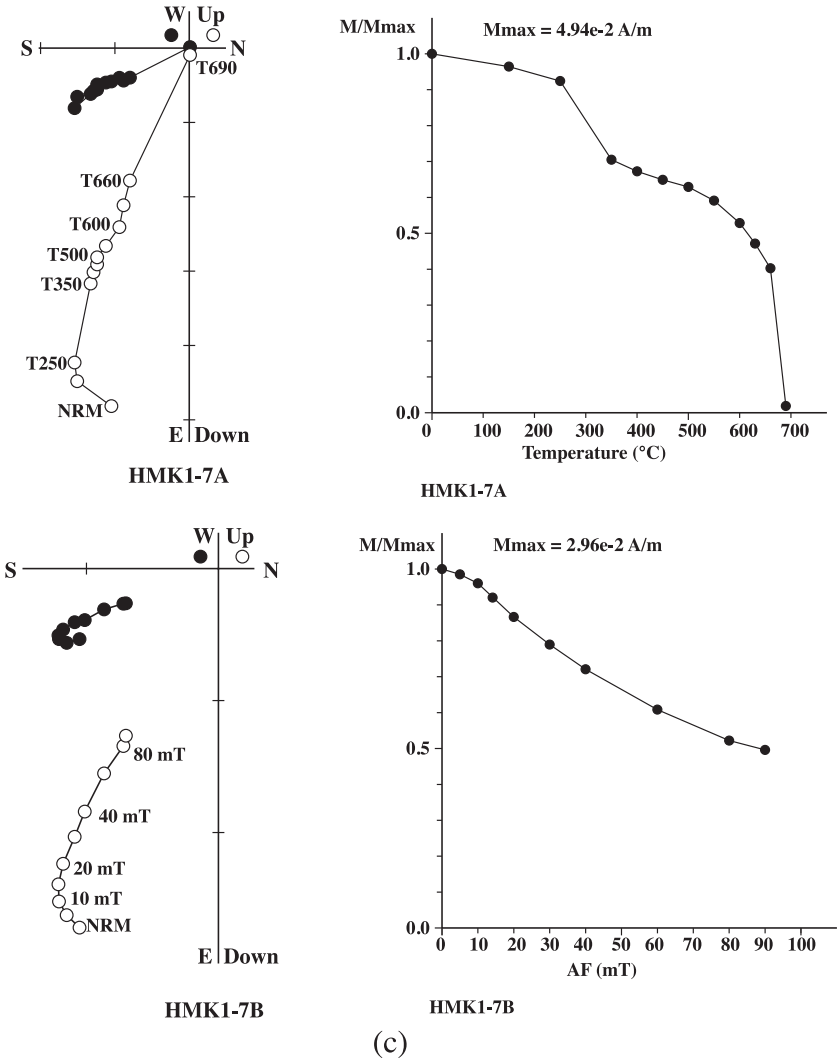

(c)

Figure 6. (*Continued.*)

mean direction of $D_g = 130.0^o$, $I_g = 57.1^o$ ($\alpha_{95} = 13.3^o$, $k = 12.8$, $N = 11$) and that for tectonic-corrected coordinates is $D_s = 143.4^o$, $I_s = 58.8^o$ ($\alpha_{95} = 9.7^o$, $k = 23.0$, $N = 11$) are obtained (red star symbol in Fig. 7, Table 1). The Fischer (1953) precision parameter (k) increases from 12.8° to 23.0°, while the 95 per cent confidence interval decreases from 13.3° to 9.7° in tectonic-corrected coordinates. Seven sites have horizontal bedding attitudes, while four sites have gently tilting attitudes, as a result we have applied the McFadden (1990) fold test. The test results in statistical parameter ξ_2 of 6.99 in geographic coordinates that is greater than the critical value of the statistical parameter ξ_c of 3.865 and 5.378 at 95 and 99 per cent confidence level, respectively. This result implies that the *in situ* average is correlated to bedding and the palaeomagnetic directions were acquired shortly after deposition.

Besides for consistency purposes, we have made comparison of our tilt-corrected pole position with previous results from Africa such as data from Dwyka System from South Africa (Opdyke *et al*. 2001), Jebel Nehoud ring complex in Kordofan, central Sudan (Bachtadse *et al*. 2002) and with the Gondwana poles for 260–320 Ma ages window (McElhinny *et al*. 2003). Fig. 8 shows details of this comparison; our data are consistent with all of the above data and particularly strongly coincident with the palaeomagnetic pole of Dwyka System of South Africa, suggesting that they are most likely contemporary.

Virtual geomagnetic poles (VGPs) for the 11 sites were then calculated (Fig. 9) and an overall mean *in situ* palaeomagnetic pole position of $\text{Lon}_g = 257.5^o\text{E}$, $\text{Lat}_g\text{s} = 20.2^o\text{S}$ ($A_{95} = 16.5^o$, $N = 11$), and that for tectonic-corrected coordinate $\text{Lon}_s = 249.5^o\text{E}$, $\text{Lat}_s = 26.0^o\text{S}$ ($A_{95} = 13.1^o$, $N = 11$; Fig. 9, Table 2). When these both poles are transferred to West African coordinate, they move towards the given APWP curve becoming more compatible.

5 DISCUSSION AND INTERPRETATION

5.1 Age estimation

The age of the Edaga Arbi Glacials and Enticho sandstones in Northern Ethiopia has been ambiguous. The absence of age diagnostic fossils and the presence of two possible distinct glacial events in the region preclude the distinction between Ordovician or Permo/Carboniferous age. Comparison of obtained palaeomagnetic pole position with the APWP curve for Africa is one way of

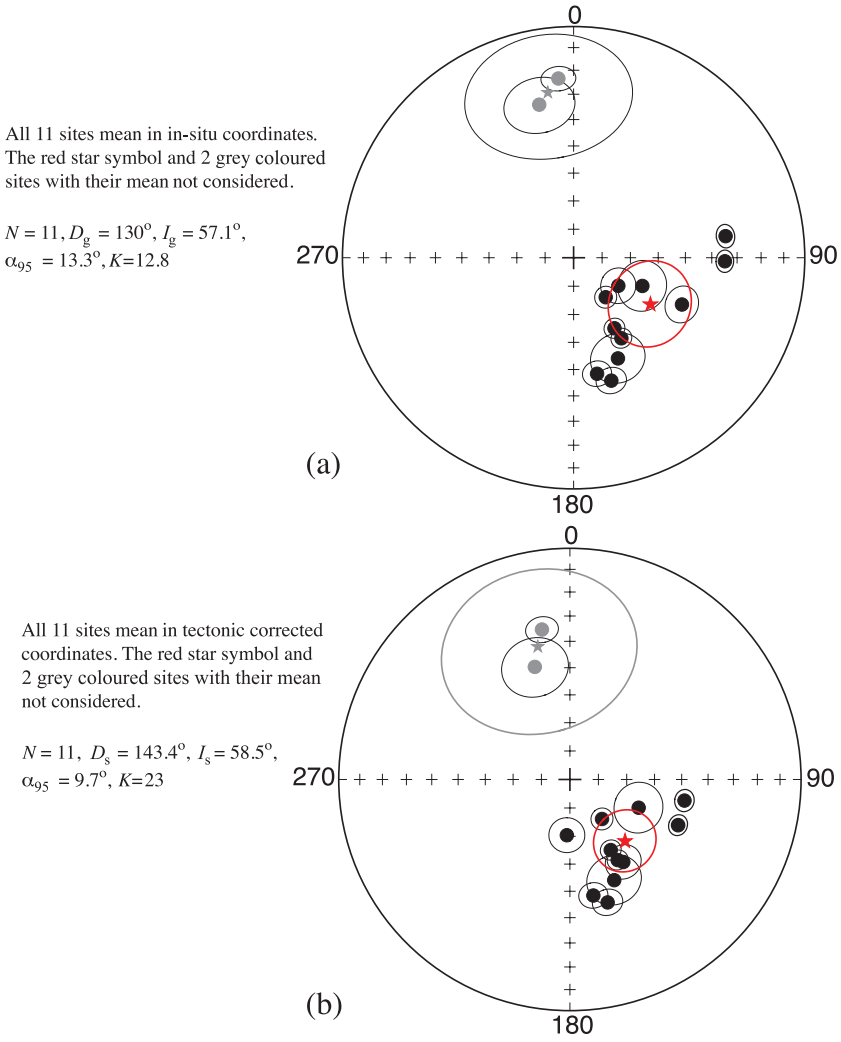

Figure 7. Stereographic projection showing site mean directions for 13 sites analysed. Two sites from coarse Enticho sandstones at Negash locality having different directions are shown in grey colours and the rest 11 sites are shown in black full circles. The overall mean directions for *in situ* coordinates (a) and tilt-corrected coordinates (b) are given. In both cases, red star symbol represents overall mean directions.

Table 1. Palaeomagnetic geographic site mean directions for the 11 averages together with over all mean directions for the Palaeozoic rocks of Ethiopia are given. Mean 1 and mean 2, respectively, indicate overall mean directions including and excluding two geographic sites where strata were tilted.

Sample name	Strike/dip	*N*	D_g	I_g	D_s	I_s	*K*	α_{95}
NBLS1	150/20	11	122.1	71.4	183.2	70.3	55.0	6.2
NBLS2	145/27	15	113.4	47.7	147.1	55.0	39.5	6.2
NBLS3	125/25	10	81.9	34.0	100.4	48.2	176.6	3.6
NPSST1	130/27	23	91.3	34.9	112.9	47.9	76.8	3.5
EPSST1	0/0	25	162.9	43.7	162.9	43.7	35.1	5.0
EPSST2	0/0	18	156.2	50.7	156.2	50.7	15.4	9.2
EDA1	0/0	13	149.9	61.1	149.9	61.1	134.4	3.6
EDA2	0/0	12	168.6	47.5	168.6	47.5	83.4	4.8
EDA3	0/0	11	149.3	56.7	149.3	56.7	164.6	3.6
HMK1	0/0	13	112.3	63.7	112.3	63.7	23.5	8.7
HMK2	0/0	13	140.9	72.1	140.9	72.1	116.8	3.9
Overall mean		11	130.0	57.1	143.4	58.5	23.0	9.7

Notes: Sample name; strike and dip, *N*, number of specimens; D_g and I_g, declination and inclination in geographic coordinates; D_s and I_s, declination and inclination in stratigraphic coordinates; *K*, Fisher precision parameter; α_{95}, 95 per cent confidence interval.

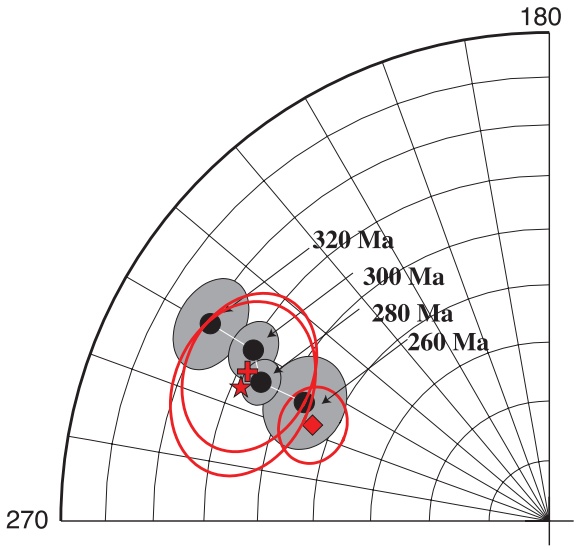

Figure 8. Comparison of our pole rotated in western coordinates (solid red star symbol) with some other poles from the region. The solid red cross symbol represents data from Dwyka system (Opdyke *et al*. 2001), the solid diamond symbol is from Jebel Nehoud ring complex in Kordofan, Sudan (Bachtadse *et al*. 2002), and also shown in McElhinny *et al*. (2003) Gondwana APWP data for time interval between 260 and 320 Ma.

testing or determining past relative positions of continents. Fig. 10(a) shows spherical projection with the APWP curve of Africa in north western African coordinates for the last 310 Ma as compiled by Besse & Courtillot (1991, 2003) and Cogné (2003) and the obtained palaeomagnetic pole position for the Palaeozoic rocks of this study. Red coloured open diamond and star symbols represent the obtained palaeomagnetic pole in the *in situ* and tilt-corrected coordinate, respectively, both in Northeast African coordinate. Red coloured full diamond and star symbols represent pole in the *in situ* and tilt-corrected coordinate, respectively, both transferred in West African coordinates. The obtained *in situ* pole position from Northern Ethiopia is shown in open red diamond symbol (Fig. 10a, Table 2), while the tilt-corrected pole position is shown in open red star symbol. These pole positions are rotated to co-ordinates of West Africa (full red diamond and star symbols) to allow for extensional rift system from the Benue Trough about an Euler pole at 19.2°N, 352.6°E through an angle −6.3° (clockwise) (Lottes & Rowley 1990; McElhinny *et al*. 2003). The transferred *in situ* pole position is located at $\mathrm{Lon_g} = 255.2^{\circ}\mathrm{E}$, $\mathrm{Lat_g} = 26.1^{\circ}\mathrm{S}$ ($A_{95} = 16.5^{\circ}$), and that for tectonic corrected is $\mathrm{Lon_s} = 246.6^{\circ}\mathrm{E}$, $\mathrm{Lat_s} = 31.8^{\circ}\mathrm{S}$ ($A_{95} = 13.1^{\circ}$) (full red diamond and star symbols, respectively, Fig. 10a). The transferred tectonic-corrected pole position is the most consistent with the APWP curve and with its 95 per cent confidence circles intersects the path in the 270–310 Ma segment and hence is compatible with an age between late Carboniferous and early Permian. In addition, our obtained tilt-corrected pole position is transferred in South African coordinates ($\mathrm{Lon_s} = 249.2^{\circ}\mathrm{E}$, $\mathrm{Lat_s} = 26.4^{\circ}\mathrm{S}$, $A_{95} = 13.1^{\circ}$, $N = 11$) about an Euler pole position, at 40.5°E, 298.6°S, through an angle 0.7° (Torsvik & Cocks 2004; Torsvik *et al*. 2008) and compared with APWP curve of Gondwana (Torsvik *et al*. 2012). This comparison considered the 95 per cent confidence circles slightly overlaps with APWP corresponding to ages of between 260 and 280 Ma, while it bears no similarity with the APW path before 290 Ma (Fig. 10b).

Both these results indicate that the Palaeozoic glacial sediments of Ethiopia have an age between 270 and 310 Ma, which is compatible with the assigned age of latest Carboniferous—early Permian period based on Palynomorphs from the glacigenic sediments (Bussert & Schrank 2007). However, the claim by Bussert & Schrank (2007) that the lower part of the Enticho sandstone is Ordovician in age is refuted by this study as palaeomagnetic directions from both the Edaga Arbi Tillite and Enticho Sandstone are not statistically different and that any existing age difference is only stratigraphic. Because our obtained pole position is strongly coincident with palaeomagnetic pole of Dwyka System from South Africa (Opdyke *et al*. 2001), the glaciogenic sediments in Northern Ethiopia are equivalent to the Dwyka sediments of Southern Africa, also consistent with south–north striations widespread in these areas. This implies that the late Carboniferous Dwyka land ice sheet had probably extended further north than previously known and that the age of the sediments is probably older than 300 Ma, consistent with various age estimates for Dwyka group sediments, formed during the Karoo Ice ages, in the Karoo region of South Africa (Hambrey & Harland 1981; Deynoux *et al*. 1994; Rubidge 2005; Selden & Nudds 2011).

6 CONCLUSIONS

Rock magnetic, microscopic studies and demagnetization behaviour of the glaciogenic sediments of Northern Ethiopia vindicated that they retained original magnetization of high quality, carried dominantly by detrital haematite. When the overall *in situ* and tectonic-corrected coordinates are determined; the precision parameter (k) increases, while the 95 per cent confidence interval decreases in bedding corrected coordinates yielding a positive fold test (McFadden 1990).

The palaeomagnetic pole position from the glacial sediment in this study is remarkably coincident with a palaeomagnetic pole of the Dwyka System from south Africa (Opdyke *et al*. 2001), with the Gondwana APWP curve with ages of between 260 and 320 Ma (Besse & Courtillot 1991, 2002; McElhinny *et al*. 2003), and also agree with the palaeomagnetic pole position obtained from igneous rocks of the Jebel Nehoud ring Complexes of Kordofan, South Sudan (Bachtadse *et al*. 2002). Comparison of this palaeomagnetic pole position with the current APWP curve for West Africa gives ages ranges of between ≈270 and 310 Ma, assigning ages of Early Permian and Late Carboniferous. The result also implies that the Late Carboniferous Dwyka land ice sheet had probably extended more than 1000 km further north than previously known and agrees with the widespread south–north oriented basins and also furrow structures reported in the Palaeozoic rocks outcrops, Northern Ethiopia.

The data being better quality and coming from North Eastern Africa where no data were previously reported potentially contribute solving earlier ambiguities on early Permian—late Carboniferous palaeomagnetic data of Gondwana and potentially contribute towards the new road of reconciliations as more data are produced from this part of the world.

ACKNOWLEDGEMENTS

We are very grateful for the fellowship support from Alexander von Humboldt Fellowship that made this investigation possible. We also thank the Research and Publication office of the Addis Ababa University for funding the field work. We are very grateful to Andy Biggin and two anonymous reviewers for their constructive comments that improved the manuscript.

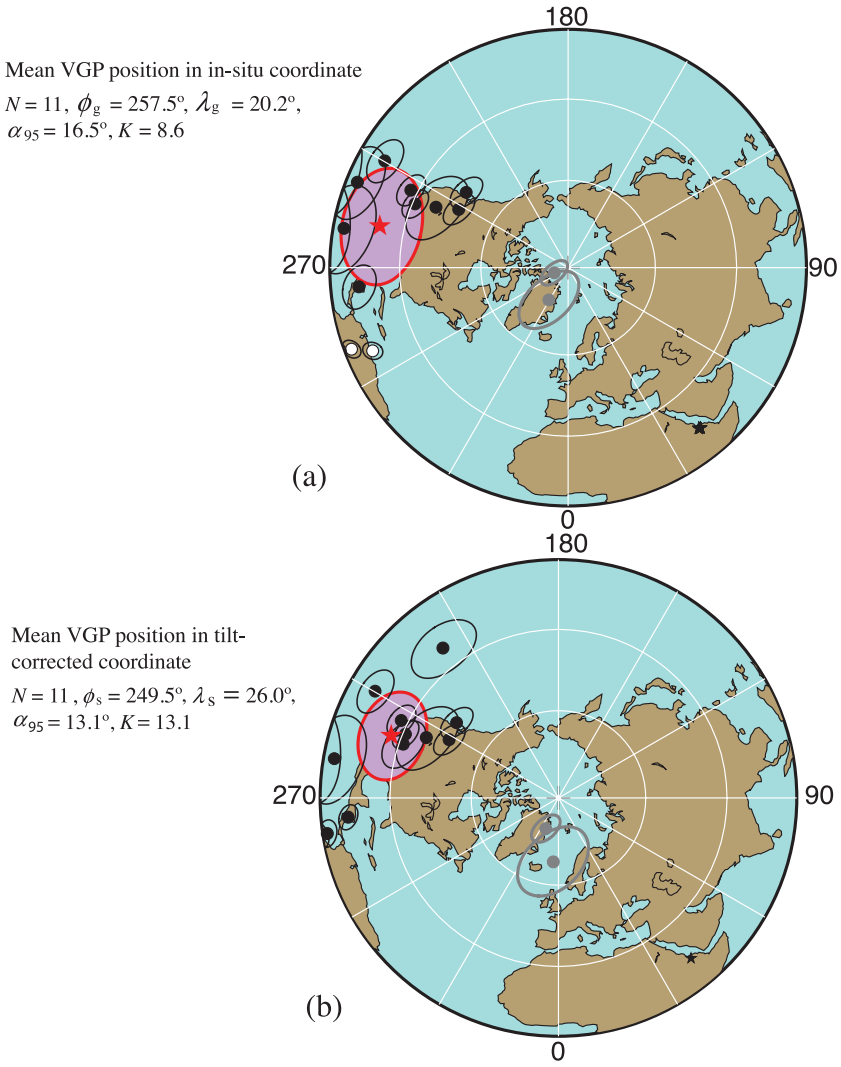

Figure 9. Stereographic projections (projected on to vertical plane) of the virtual geomagnetic pole (VGP) of all the 13 site mean directions are given. The VGPs of the two sites from coarse Enticho sandstones at Negash locality having different directions are shown in grey colours. The VGP for the rest 11 sites is shown in black full circles for which overall mean palaeomagnetic pole positions were calculated (red star symbol); (a) *In situ* coordinate and (b) tilt-corrected coordinate.

Table 2. Site mean VGPs for the 11 averages together with the overall mean pole position for the Palaeozoic rocks of Ethiopia are given. In addition, obtained pole was transferred to the West Africa coordinates and values are given as ROTPOLE.

Sample name	Strike/dip	*N*	ϕ_g	λ_g	ϕ_s	λ_s	*K* (d*p*)	α_{95} (d*m*)
NBLS1	150/20	11	247.9	5.2	217.6	21.7	9.3	10.7
NBLS2	145/27	15	275.2	12.9	250.9	31.6	6.2	8.7
NBLS3	125/25	10	293.1	-11.9	278.8	2.1	3.1	4.8
NPSST1	130/27	23	290.6	-3.3	275.2	12.4	3.0	4.5
EPSST1	0/0	25	241.9	46.9	241.9	46.9	3.9	6.2
EPSST2	0/0	18	245.4	38.9	245.4	38.9	8.3	12.4
EDA1	0/0	13	243.8	27.3	243.8	27.3	4.2	5.5
EDA2	0/0	12	233.5	45.8	233.5	45.8	4.0	6.2
EDA3	0/0	11	247.4	31.1	247.4	31.1	3.7	5.2
HMK1	0/0	13	260.1	5.1	260.1	5.1	11.0	13.9
HMK2	0/0	13	239.8	12.0	239.8	12.0	6.0	6.8
Overall mean		11	257.5	20.2	249.5	26.0	13.1	13.1

Notes: Sample name; strike/dip; *N*, number of samples; ϕ_g and λ_g, pole longitude and latitude in geographic coordinates; ϕ_s and λ_s pole longitude and latitude in stratigraphic coordinates; *K* (d*p*), Fisher precision parameter; α95, 95 per cent confidence interval. The overall mean VGPs directions are calculated for sites ($N = 11$).

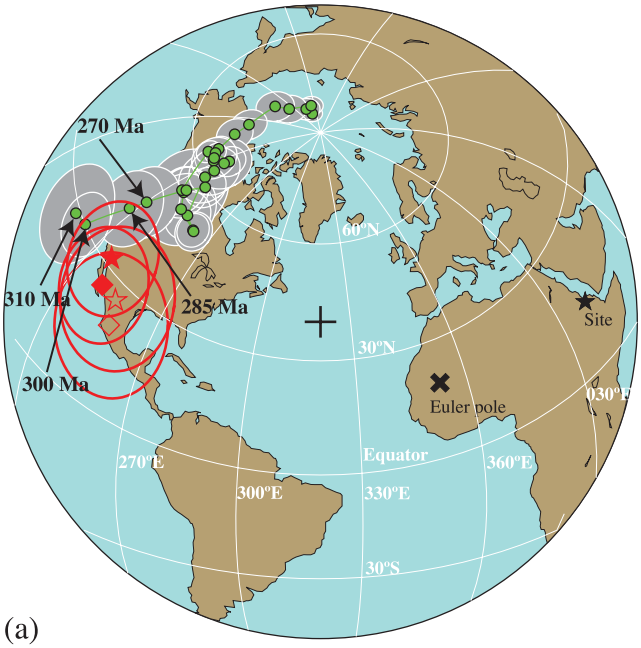

(a)

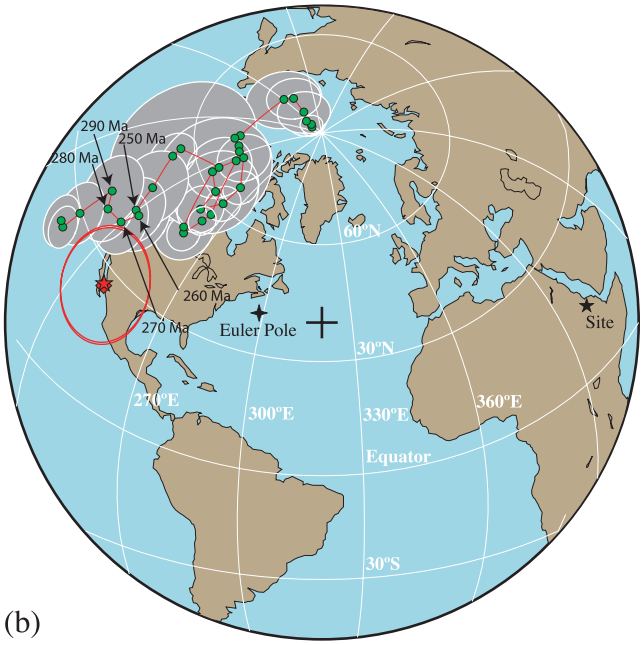

(b)

Figure 10. (a) Spherical projections with the major plates in their present-day configurations and the APWP curve of Africa in West African coordinates (Besse & Courtillot 1991, 2002, 2003; McElhinny *et al*. 2003) is given. Our obtained pole position is given in red coloured diamond and star symbols in north–east African and west African coordinate about Euler pole position in black coloured cross symbol. The open diamond and star symbols represent the data *in situ* and after tectonic correction, respectively. The rotated pole is consistent with ages of 270–310 Ma. (b) Spherical projections with the major plates in their present-day configurations and the APWP curve of Gondwana in South African coordinates (Torsvik *et al*. 2012) are given. Our obtained pole position for the sample site in East Africa (black star) is shown in red diamond symbol and the red star symbol represents the geomagnetic pole after transferred in to the south African coordinate about Euler pole position shown in four-leg star symbol. The 95 per cent confidence circle of both poles slightly cut APWP curve at ages of 250–300 Ma.

REFERENCES

Bachtadse, V., Zänglein, R., Tait, J. & Soffel, H.C., 2002. Paleomagnetism of the permo/carboniferous (280 Ma) Jebel Nehoud ring complex, Kordofan, Central Sudan, *J. Afr. Earth Sci.,* **35,** 89–97.

Besse, J. & Courtillot, V., 1991. Revised and synthetic apparent polar wander paths of the African, Eurasian, North American and Indian plates, and true polar wander since 200 Ma, *J. geophys. Res.,* **96,** 4029–4050.

Besse, J. & Courtillot, V., 2002. Apparent and true polar wander and the geometry of the geomagnetic field over the last 200 Myr, *J. geophys. Res.,* **107**(B11), 2300, doi:10.1029/2000JB000050.

Besse, J. & Courtillot, V., 2003. Correction to "Apparent and true polar wander and the geometry of the geomagnetic field over the last 200 Myr," *J. geophys. Res.,* **108**(B10), 2469, doi:10.1029/2003JB002684.

Beuf, S., Biju-Duval, B., de Charpel, O., Rognon, P., Gariel, O. & Bennacef, A., 1971. *Les Grès du Paléozoique Inférieur au Sahara: Sedimentation et Discontinuities Évolution Structurale d'un Craton*, Technip.

Beyth, M., 1972a. To the geology of Central-Western Tigre, *Dissertation*, Rheinische Friedrichs-Wilhelms-Universitat Bonn, Bonn, p. 155.

Beyth, M., 1972b. Paleozoic–Mesozoic sedimentary basin of Mekele Outlier, Northern Ethiopia, *Bull. Am. Assoc. Petrol. Geol.,* **56,** 2426–2439.

Beyth, M., 1973. Correlation of Palaeozoic–Mesozoic sediments in Northern Yemen and Tigre, Northern Ethiopia, *Bull. Am. Assoc. Petrol. Geol.,* **57,** 2440–2443.

Blanford, W.T., 1869. On the geology of a portion of Abyssinia, *J. geol. Soc. Lond.,* **25,** 401–406.

Blanford, W.T., 1870. *Observations on the Geology and Zoology of Abyssinia*, Mcmillan & Co., p. 487.

Bussert, R. & Schrank, E., 2007. Palynological evidence for a latest Carboniferous-Early Permian glaciation in Northern Ethiopia, *J. Afr. Earth Sci.,* **49,** 201–210.

Clark-Lowes, D.D., 2005. Arabian glacial deposits: recognition of palaeovalleys within the Upper Ordovician Sarah Formation, Al Qasim district, Saudi Arabia, *Proc. Geol. Assoc.,* **116,** 331–347.

Cogné, J.P., 2003. PaleoMac: a Macintosh^{TM} application for treating paleomagnetic data and making plate reconstruction, *Geochem. Geophys. Geosyst.,* **4**(1), 1007.

Deynoux, M., Miller, J.M.G. & Domack, E.W., 1994. *Earth's Glacial Records*, Cambridge University Press, 266 pp.

Domeier, M., Van der Voo, R. & Torsvik, T.H., 2012. Paleomagnetism and Pangea: the road to reconciliation, *Tectonophysics,* **514–517,** 14–43.

Dow, D.B., Beyth, M. & Hailu, T., 1971. Palaeozoic glacial rocks recently discovered in northern Ethiopia, *Geol. Mag.,* **108,** 53–60.

Du Toit, A.L., 1953. *The Geology of South Africa*, Hafner. Pub. Co.

Fischer, R.A., 1953. Dispersion on a sphere, *Proc. R. Soc. Lond., Ser. A.,* **217,** 295–305.

Furon, R., 1963. *Geology of Africa*, Hafner. Pub. Co.

Halls, H.C., 1976. A least-squares method to find a remanence direction from converging remagnetization circles, *Geophys. J. R. astr. Soc.,* **45,** 297–304.

Halls, H.C., 1978. The use of converging remagnetization circles in paleomagnetism, *Phys. Earth planet. Inter.,* **16,** 1–11.

Hambrey, M.J. & Harland, W.B., 1981. Earth's pre–Pleistocene Glacial Record, International Geological Programme, *Project 38: Pre–Pleistocene Tillite,* P76.

Hallam, A., 1983. Supposed Permo-Triassic megashear between Laurasia and Gondwana, *Nature,* **301**(5900), 499–502.

Irving, E., 1977. Drift of the major continental blocks since the Devonian, *Nature,* **270,** 304–309.

Kanasewich, E.R., Havskov, J. & Evans, M.E., 1978. Plate tectonics in the Phanerozoic. *Can. J. Earth Sci.,* **15**(6), 919–955.

Kirschvink, J.L., 1980. The least squares line and plane and the analysis of paleomagnetic data, *Geophys. J. R. astr. Soc.,* **62,** 699–718.

Klitgord, K.D. & Schouten, H., 1986. Plate kinematics of the Central Atlantic, in *The Geology of North America: The Western North Atlantic Region*, eds Vogt, P.R. & Tucholke, B.E., Geol. Soc. Am.

Krasa, D., Petersen, K. & Petersen, N., 2007. The variable field translation balance, in *Encyclopedia of Geomagnetism and paleomagnetism: Dordrecht*, pp. 977–979, eds Gubbins, D. & Herrero-Bervera, E., Springer.

Lottes, A.L. & Rowley, D.B., 1990. Early and Late Permian reconstructions of Pangaea, in *Paleozoic Paleogeography & Biogeography*, Vol. 12, pp. 383–395, eds McKerrow, W.A. & Scotese, C.R., Geol. Soc. Mem.

McElhinny, M.W. & McFadden, P.L., 2000. *Paleomagnetism Continents and Oceans*, Academic Press, 386 pp.

McElhinny, M.W., Briden, J.C., Jones, D.L., Brock, A., 1968. Geological and geophysical implications of paleomagnetic results from Africa, *Rev. Geoph.,* **6**(2), 201–238.

McElhinny, M.W., Powell, McA, C. & Pisarevsky, S.A., 2003. Paleozoic terranes of eastern Australia and the draft history of Gondwana, *Tectonophysics,* **362,** 41–65.

McFadden, P.L., 1990. A new fold test for paleomagnetic studies, *Geophys. J. Int.,* **103,** 163–169.

McFadden, P.L. & McElhinny, M.W., 1988. The combined analysis of remagnetization circles and direct observations in paleomagnetism, *Earth planet. Sci. Lett.,* **87,** 152–160.

Merla, G. & Minucci, E., 1938. *Mission Geologica Nel Tigrai*, Roma Real Accadema d'Italia.

Mohr, P.A., 1965. *The Geology of Ethiopia*, Poligrafico.

Moreau, J., Ghienne, J.-F., Le Heron, D.P., Rubino, J.-L. & Deynoux, M., 2005. 440 Ma ice stream in North Africa, *Geology,* **33,** 753–756.

Morel, P. & Irving, E., 1981. Paleomagnetism and the evolution of Pangea, *J. geophys. Res.,* **86**(B3), 1858–1872.

Muttoni, G., Kent, D.V., Garzanti, E., Brack, P., Abrahamsen, N. & Gaetani, M., 2003. Early Permian Pangea "B" to Late Permian Pangea "A", *Earth. planet. Sci. Lett.,* **215**(3–4), 379–394.

Muttoni, G. *et al.*, 2009. Opening of the Neo-Tethys Ocean and the Pangea B to Pangea A transformation during the Permian, *GeoArabia,* **14**(4), 17–48.

Opdyke, N.D., Mushayandebvu, M. & de Wit, M.J., 2001. A new paleomagnetic pole for the Dwyka System and correlative sediments in sub-Saharan Africa, *J. Afr. Earth Sci.,* **33,** 143–153.

Rochette, P. & Vandamme, D., 2001. Pangea B; an artifact of incorrect paleomagnetic assumptions?, *Ann. Geofisica.,* **44,** 649–658.

Rubidge, B.S., 2005. Re–uniting lost continents – fossil reptiles from the ancient Karoo and their wanderlust, *South Afr. J. Geol.,* **108**(1), 135–172.

Sacchi, R., Alene, M., Barbieri, M. & Conti, A., 2007. On the Paleozoic Tillite of the Adigrat Group (Tigrai, Ethiopia), *Per. Mineral,* **76**(2–3), 241–251.

Saxena, G.N. & Assefa, G., 1983. New evidence on the age of the glacial rocks of northern Ethiopia, *Geol. Mag.,* **120,** 549–554.

Selden, P. & Nudds, J., 2011. *Karoo. Evolution of Fossil Ecosystems*, 2nd edn, Manson Publishing, pp. 104–122.

Semtner, A.K. & Klitzsch, E., 1994. Early Paleozoic paleogeography of the northern Gondwana margin: new evidence for Ordovician-Silurian glaciation, *Geol. Rundschau,* **83,** 743–751.

Shackleton, R.M. & Lomax, K., 1974. Paleomagnetic evidence for the Permian age of tillites in Ethiopia, *Research Institute of African Geology, University of Leeds, Annual Report*, No. 18, p. 13.

Smith, A.G. & Livermore, R.A., 1991. Pangea in Permian to Jurassic time, *Tectonophysics,* **187**(1–3), 135–179.

Torsvik, T.H. & Cocks, L.R.M., 2004. Earth geography from 400 to 250 Ma: a paleomagnetic, faunal and facies review, *J. geol. Soc.,* **161,** 555–572.

Torsvik, T.H., Müller, R.D., Van der Voo, R., Steinberger, B. & Gaina, C., 2008. Global Plate motion frames: toward a unified model, *Rev. Geophys.,* **46,** RG3004, doi:10.1029/2007RG000227.

Torsvik, T.H. *et al.*, 2012. Phanerozoic polar wander, paleogeography and dynamics, *Earth Sci. Rev.,* **114,** 325–368.

Van der Voo, R., 1993. *Paleomagnetism of the Atlantic Tethys, and Iapetus Oceans*, Cambridge University Press, 411 pp.

Vaslet, D., 1990. Upper Ordovician glacial deposits in Saudi Arabia, *Episodes,* **13,** 147–161.

Wegener, A., 1915. *Die Entstehung der Kontinente und Ozeane*, Sammlung Vieweg, 94 pp.